

## Density-activated defect recombination as a possible explanation for the efficiency droop in GaN-based diodes

J. Hader,<sup>1,a)</sup> J. V. Moloney,<sup>1</sup> and S. W. Koch<sup>2</sup>

<sup>1</sup>Nonlinear Control Strategies Inc., 3542 N. Geronimo Ave., Tucson, Arizona 85705, USA and Optical Sciences Center, University of Arizona, Tucson, Arizona 85721, USA

<sup>2</sup>Department of Physics and Materials Sciences Center, Philipps Universität Marburg, Renthof 5, 35032 Marburg, Germany

(Received 16 April 2010; accepted 14 May 2010; published online 3 June 2010)

It is shown that a carrier loss process modeling density-activated defect recombination can reproduce the experimentally observed droop of the internal quantum efficiency in GaN-based laser diodes. © 2010 American Institute of Physics. [doi:10.1063/1.3446889]

GaN-based light emitting diodes for the blue-green wavelength regime are known to suffer from the so-called “efficiency droop.” The internal quantum efficiency peaks at very low pump currents (typically  $<10$  A/cm<sup>2</sup>) and then drops significantly for currents desired for applications like general illumination or projection displays (hundreds of ampere per square centimeter).<sup>1,2</sup> The physical processes causing the droop are still under intense debate.

The internal quantum efficiency,  $\eta_i$ , is defined as follows:

$$\eta_i = \frac{J_{\text{rad}}}{J_{\text{loss}}}, \quad (1)$$

where  $J_{\text{rad}}$  is the portion of the injected current that is converted into photons and  $J_{\text{loss}}$  is the total injected current which is usually separated into the following:

$$J_{\text{loss}} = J_{\text{defect}} + J_{\text{rad}} + J_{\text{aug}} + J_{\text{rest}}. \quad (2)$$

Here,  $J_{\text{defect}}$  is the loss current due to carrier recombination via defects which is commonly assumed to scale linearly with the carrier density,  $N$ .  $J_{\text{aug}}$  is the loss current due to Auger processes.<sup>3</sup>  $J_{\text{rest}}$  comprises all remaining loss processes like current leakage or noncapture of carriers.

Experimentally, the individual contributions to the loss current cannot be determined separately. A common approach therefore is to fit a power-law expansion to the measured density dependence of the loss current and to associate the linear, quadratic and cubic terms with the defect-, radiative-, and Auger-loss processes, respectively. In Refs. 2 and 4, such a procedure was used and good fits to measured efficiencies were obtained assuming a significant contribution of the cubic term. Thus, it was argued that Auger processes are responsible for the droop.

Our current, state of the art theoretical calculations find that the Auger rates in these wide-gap materials are generally too small to explain the droop. Whereas loss rates due to the direct intraband Auger processes have been found orders of magnitude too small,<sup>5</sup> it has been argued that interband Auger processes may yield the necessary magnitude.<sup>6</sup> However, this requires that the energy separation between the higher and lower bulk bands is very close to the fundamental band gap—which, in general, is not the case. Our own preliminary calculations furthermore show that also phonon-assisted Au-

ger processes are typically not strong enough to generally explain the droop. Thus, to date, the only genuine indication that Auger processes might be responsible for the droop is the observation that the measured efficiencies can be well fitted assuming a loss process with an  $N^3$ -dependence.

In this letter, we propose an alternative explanation for the droop. We argue that a loss process with an alternative density dependence can also reproduce the experimental observations. We speculate that this loss process is caused by density-activated defect recombination (DADR).

The physical model behind our concept is depicted schematically in Fig. 1. At low pump currents and correspondingly low carrier densities, electrons, and holes occupy states in local in-plane potential minima. These minima are caused

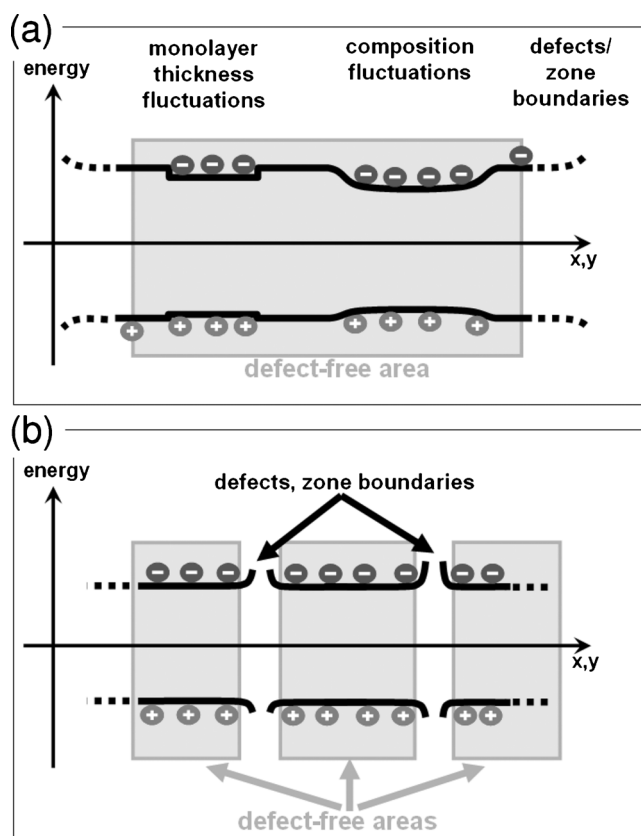


FIG. 1. Schematic sketch of in-plane potential variations due to local well width fluctuations and composition fluctuations (a) or due to local energy-activated defect states (b).

<sup>a)</sup>Electronic mail: jhader@acms.arizona.edu.

by fluctuations in the well composition and/or by well-width fluctuations. With increasing density, carriers gradually escape from these minima and start to fill the entire quantum well. If, as depicted in Fig. 1(a), the regions of the potential minima are relatively defect free and locally separated from areas of high defect density and/or strong defect recombination centers, density activated defect recombination occurs at elevated densities where the carriers leave the potential minima. The same effect would be observed if the recombination centers are surrounded by potential barriers [Fig. 1(b)].

The details of the local distribution and potential shapes of defect recombination centers in GaN-based materials are not known with high accuracy. However, transmission electron microscopy and atomic force studies show fairly large composition fluctuations and indicate that the recombination centers are indeed distributed inhomogeneously and mainly located in regions with elevated potential.<sup>7-9</sup> Thus, the scenarios depicted in Fig. 1 do seem plausible.

Motivated by these observations, we propose the following simple density dependence for the DADR loss current:

$$J_{\text{DADR}} = \begin{cases} 0, & \text{for } N < N_0 \\ \frac{en_w}{\tau_{\text{DADR}}} \frac{(N - N_0)^2}{2N_0}, & \text{for } N > N_0 \end{cases} \quad (3)$$

Here,  $n_w$  is the number of wells and  $N$  and  $N_0$  are sheet carrier densities per well. The recombination time,  $\tau_{\text{DADR}}$ , and density at which the DADR sets on,  $N_0$ , are determined by a fit to the experimental data.

One factor  $(N - N_0)$  in Eq. (3) represents the linear density dependence usually associated with defect recombination processes. The second factor  $(N - N_0)$  accounts for the increasing number of recombination centers that become available at elevated densities. While the correct dependence of the second factor is probably more complex, we use the simplest form here, resulting in an overall  $(N - N_0)^2$ -dependence.

Making the assumption that Auger recombination can be completely neglected, the total loss current in our model is given by the following:

$$J_{\text{loss}} = J_{\text{defect}} + J_{\text{rad}} + J_{\text{DADR}}. \quad (4)$$

Here,  $J_{\text{defect}}$  is the recombination due to those defects that might be present also in the potential minima. For this overall spatially homogeneous loss, we assume the usual linear density dependence,  $J_{\text{defect}}(N) = en_w N / \tau_d$ . The radiative contribution is calculated using our fully microscopic many-body theory as described in Ref. 5.

The potential variations are assumed to be statistically distributed both in location and in height. This leads to a statistical distribution of carrier densities. We model this by applying a Gaussian broadening to the currents in the form of the following:

$$J(N) = \frac{1}{\sqrt{2\pi\sigma^2}} \int_0^\infty d\tilde{N} J(\tilde{N}) e^{-(N - \tilde{N})^2/2\sigma^2}, \quad (5)$$

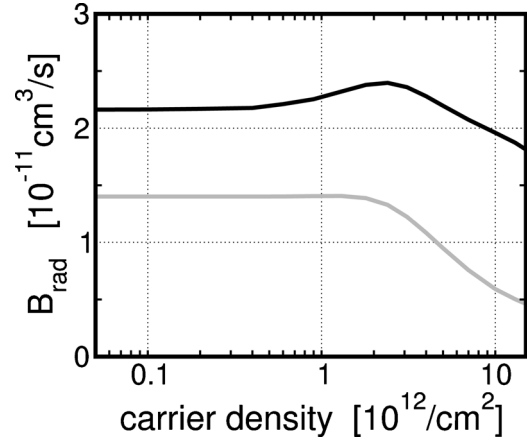


FIG. 2. Microscopically calculated radiative loss coefficient as function of the sheet carrier density per well. The results for the 410 nm device from Ref. 4 are shown in black and for the 530 nm device from Ref. 10 in gray.

$$\tilde{N}(N) = N \left( \frac{1}{\sqrt{2\pi\sigma^2}} \int_0^\infty dN' N' e^{-(N - N')^2/2\sigma^2} \right)^{-1}. \quad (6)$$

Here we introduce the renormalized density  $\tilde{N}$  for density conservation. The half width at half maximum (HWHM) of the broadening is given by  $\sqrt{2\sigma^2 \ln 2}$ .

To a certain extent this also models an exponential onset of the DADR according to carriers in the high energy tails of the carrier distributions reaching the defects first.

To test this model, we analyze the experimentally measured efficiencies reported in Ref. 4 for a device operating around 410 nm and in Ref. 10 for a device around 530 nm. The structure for 410 nm contains four 3 nm wide  $\text{In}_{0.1}\text{Ga}_{0.9}\text{N}/\text{GaN}$  wells. The structure for 530 nm operation contains only one well. Although it is not unambiguously clear from the publication, we assume this to be a 2 nm wide  $\text{InGaIn}/\text{GaN}$ -well.

Figure 2 shows the microscopically calculated radiative loss coefficient,  $B_{\text{rad}} = J_{\text{rad}} w_w / (en_w N^2)$ , where  $w_w$  is the well width. In both structures, the density dependence of the radiative loss becomes less than quadratic at high densities due to phase space filling.<sup>3</sup> In the low density limit  $B_{\text{rad}} \approx 2.25 \times 10^{-11} \text{ cm}^3/\text{s}$  for the 410 nm structure which is similar to the number used in Ref. 4.

Figure 3 shows the fits to the experimental efficiencies using the DADR model. For the 410 nm structure, Fig. 3(a), we assumed a recombination time of  $\tau_d = 36 \text{ ns}$  for  $J_{\text{defect}}$ . For the DADR we used  $N_0 = 10^{12} \text{ cm}^{-2}$  and  $\tau_{\text{DADR}} = 3.8 \text{ ns}$ . For the best fit we applied a broadening with a HWHM of  $3.5 \times 10^{11} \text{ cm}^{-2}$ . For the 530 nm structure, [Fig. 3(b)], we find the best fit for  $\tau_d = 50 \text{ ns}$ ,  $N_0 = 0.26 \times 10^{12} \text{ cm}^{-2}$ ,  $\tau_{\text{DADR}} = 3.7 \text{ ns}$  and a broadening with HWHM of  $3.0 \times 10^{11} \text{ cm}^{-2}$ .

The defect recombination times,  $\tau_d$ , are in the range usually quoted for similar structures if Auger losses are assumed to be significant.<sup>2,4</sup> The much shorter DADR times are in the range usually quoted for  $\tau_d$  in such structures if it is assumed that Auger is not relevant.<sup>11</sup>

The broadening according to local density variations is rather unimportant for the 410 nm structure. In the 530 nm structure, the best fit is achieved for a similar broadening as in the 410 nm structure. Here, it leads to a significantly better fit, especially near the onset of the droop. We also find that we cannot achieve a very good fit at low currents if we do

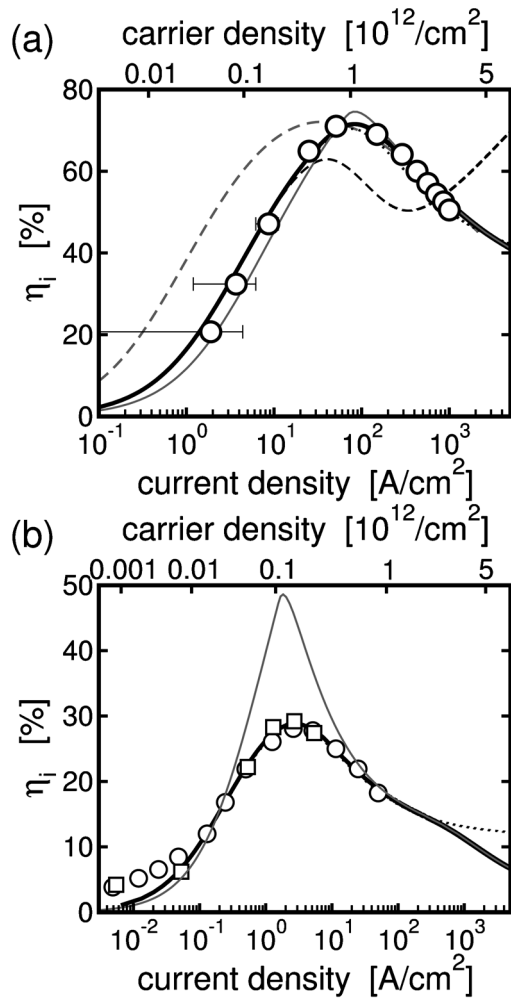


FIG. 3. Internal efficiencies as function of the current-density at 300 K. (a) and (b) experimental data from Refs. 4 and 10. Circles/squares: experimental data for electrical/resonant optical excitation. Solid black line: theory assuming DADR with a  $(N-N_0)^2$  dependence. The listed carrier densities are for this case. Solid gray line: without broadening of the loss currents. Dotted line: assuming  $B_{\text{rad}}(N)=B_{\text{rad}}(0)$ . Dashed gray line in (a) fit according to Ref. 4. Dashed black line in (a) with a  $(N-N_0)$  dependence for DADR. Horizontal bars indicate the read-out error from the graph with linear  $x$ -axis in Ref. 4.

not consider local density variations but assume a homogeneous density distribution for  $J_{\text{rad}}$  and  $J_{\text{defect}}$ . Broadening only  $J_{\text{DADR}}$  according to a variation in potentials surrounding the defects allows to get a good fit for the droop region. However, the efficiencies fall off too strongly with decreasing currents if the other currents are not broadened too. The broadening leads to an increase in the radiative losses relative to the defect losses and, thus, to a significant increase in the efficiency at low currents.

In both structures, the DADR onset density  $N_0$  leads to carrier distributions for which the dominant number of carriers is located at energies less than about 100 meV from the minimum. To create potential minima of that order requires a fluctuation of the indium composition of only about 2%–3%—which is well within the typical situation in such devices.<sup>7–9,11</sup>

Our results demonstrate that the  $(N-N_0)^2$  dependence can give excellent agreement with the experiment for all

measured densities. One could argue that in the high-density limit, DADR should switch-over to a linear density dependence. However, as shown by the dashed line in Fig. 3(a), such a dependence can reproduce the experimental results only in a limited range and fails badly at elevated densities. Here, it would even predict a switch-over to an increasing efficiency which has not been observed experimentally. For the linear dependency case the factor  $[(N-N_0)^2/N_0]$  is replaced by  $(N-N_0)$  in Eq. (3) while all other parameters are kept the same.

In real systems, it may be that other effects at high densities, such as carrier noncapture, spill-over and/or leakage ( $J_{\text{rest}}$ ) become increasingly important.<sup>12,13</sup> However, in order to avoid additional unknown fitting parameters, we did not include such features in our current simulations.

As can be seen by the dotted lines in Fig. 3, the classical assumption of a density independent  $B_{\text{rad}}$  only breaks down at densities near typical laser thresholds.

In summary, we propose DADR as a possible reason for the efficiency droop in GaN-based materials. The postulated density dependence  $\propto(N-N_0)^2$  for this process can reproduce experimentally measured efficiencies very well using plausible assumptions and parameter values. Experimentally, it has been observed that the efficiency droop is rather insensitive to the average defect density.<sup>2</sup> This has been used as an argument against defect processes as a leading cause for the efficiency droop. However, the average defect density only influences the traditional  $J_{\text{defect}}$  and should not necessarily impact the DADR which thus constitutes a viable alternative explanation for the experimental droop observations.

This work was supported by the U.S. Air Force Office of Scientific Research, Contract No. FA9550-07-1-0573, by the Deutsche Forschungsgemeinschaft and the Humboldt Foundation.

<sup>1</sup>T. Mukai, M. Yamada, and S. Nakamura, *Jpn. J. Appl. Phys., Part 1* **38**, 3976 (1999).

<sup>2</sup>Y. C. Shen, G. O. Mueller, S. Watanabe, N. F. Gardner, A. Munkholm, and M. R. Krames, *Appl. Phys. Lett.* **91**, 141101 (2007).

<sup>3</sup>J. Hader, J. V. Moloney, and S. W. Koch, *Appl. Phys. Lett.* **87**, 201112 (2005).

<sup>4</sup>M. Zhang, B. Bhattacharya, J. Singh, and J. Hinckley, *Appl. Phys. Lett.* **95**, 201108 (2009).

<sup>5</sup>J. Hader, J. V. Moloney, B. Pasenow, S. W. Koch, M. Sabathil, N. Linder, and S. Lutgen, *Appl. Phys. Lett.* **92**, 261103 (2008).

<sup>6</sup>K. T. Delaney, P. Rinke, and C. Van de Walle, *Appl. Phys. Lett.* **94**, 191109 (2009).

<sup>7</sup>K. Okamoto, A. Scherer, and Y. Kawakami, *Appl. Phys. Lett.* **87**, 161104 (2005).

<sup>8</sup>M. J. Galtrey, R. A. Oliver, M. J. Kappers, C. J. Humphreys, D. J. Stokes, P. H. Clifton, and A. Cerezo, *Appl. Phys. Lett.* **90**, 061903 (2007).

<sup>9</sup>G. H. Gu, C. G. Park, and K. B. Nam, *Phys. Status Solidi (RRL)* **3**, 100 (2009).

<sup>10</sup>A. Laubsch, M. Sabathil, J. Baur, M. Peter, and B. Hahn, *IEEE Trans. Electron Devices* **57**, 79 (2010).

<sup>11</sup>B. Witzigmann, V. Laino, M. Luisier, U. T. Schwarz, G. Feicht, W. Wegscheider, K. Engl, M. Furtisch, A. Leber, A. Lell, and V. Härle, *Appl. Phys. Lett.* **88**, 021104 (2006).

<sup>12</sup>I. A. Pope, P. M. Smowton, P. Blood, J. D. Thomson, M. J. Kappers, and C. J. Humphreys, *Appl. Phys. Lett.* **82**, 2755 (2003).

<sup>13</sup>M.-H. Kim, M. F. Schubert, Q. Dai, J. K. Kim, E. F. Schubert, J. Piprek, and Y. Park, *Appl. Phys. Lett.* **91**, 183507 (2007).